

Tropospheric ozone anomalies during El Niño
and
CO₂ retrieval from high resolution NDACC spectra
Master Thesis and PhD

Rafaella Chiarella

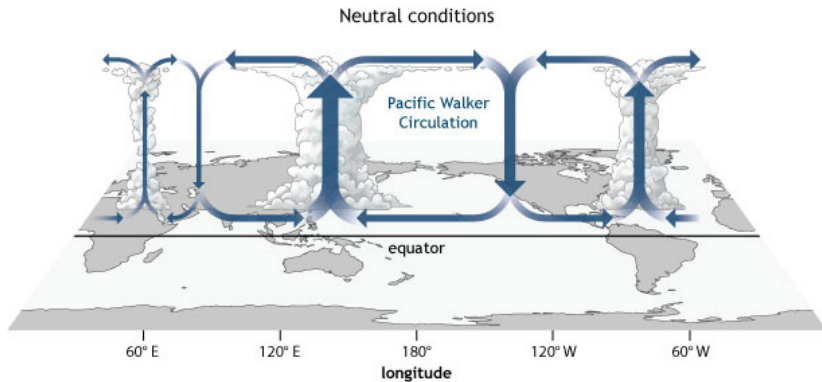
University of Bremen

12.07.2019

Outline

- 1 Tropospheric ozone anomalies during El Niño
 - Effects of El Niño in the troposphere
 - Data used
 - Results: satellite observations and simulations
 - Summary
- 2 xCO₂ retrieval from high resolution NDACC spectra
 - Introduction
 - Data and Methods
 - Results: Fit and comparisons
 - Sensitivity studies
 - Summary
- 3 Outlook

The Walker cell

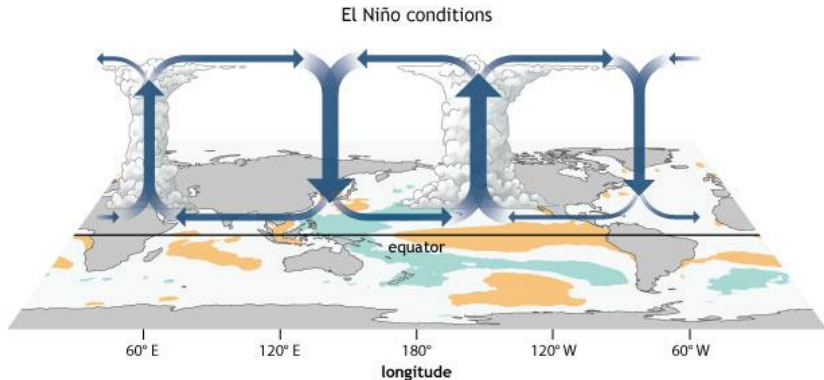


NOAA Climate.gov

Standard Walker Circulation for December-February during neutral conditions (Figure taken from NOAA: [https://www.climate.gov/news-features/blogs/ enso/walker-circulation-ensos-atmospheric-buddy](https://www.climate.gov/news-features/blogs/enso/walker-circulation-ensos-atmospheric-buddy), drawing by Fiona Martin.)

The Walker cell and El Niño

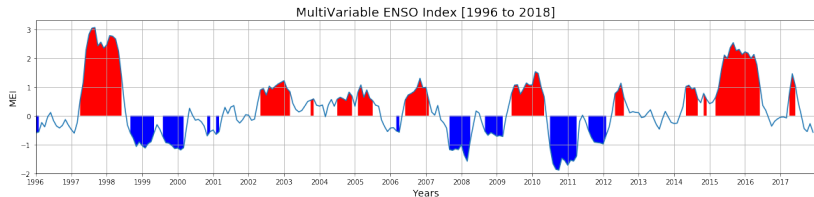
Sea Surface Temperature positive anomalies



NOAA Climate.gov

Standard Walker Circulation for December-February during El Niño conditions (Figure taken from NOAA: <https://www.climate.gov/news-features/blogs/enso/walker-circulation-ensos-atmospheric-buddy>, drawing by Fiona Martin.)

Effects of El Niño in the troposphere



Data from: <https://www.esrl.noaa.gov/psd/enso/mei/>

- Reverse of the Walker circulation, suppressed convection and drought over the Pacific warm pool [Ropelewski and Halpert, 1987].
- Higher count of wild fires on Oceania [Doherty et al., 2006].
- Increase of Tropical Tropospheric Column of Ozone (TTCO) in Pacific warm pool [Chandra et al., 1998], [Fujiwara and Kita, 2000], [Sudo and Takahashi, 2001], [Thompson, 2001].
- Other tropospheric chemistry changes [Sudo and Takahashi, 2001].

Tropical Tropospheric Ozone Column [Leventidou, 2017]

- GOME/ERS-2, SCIAMACHY/Envisat, GOME-2/MetOp-A,
- Available for 1996 to 2017 and 20°N and 20°S
- Convective Cloud Differential (CCD) [Ziemke et al., 1998]

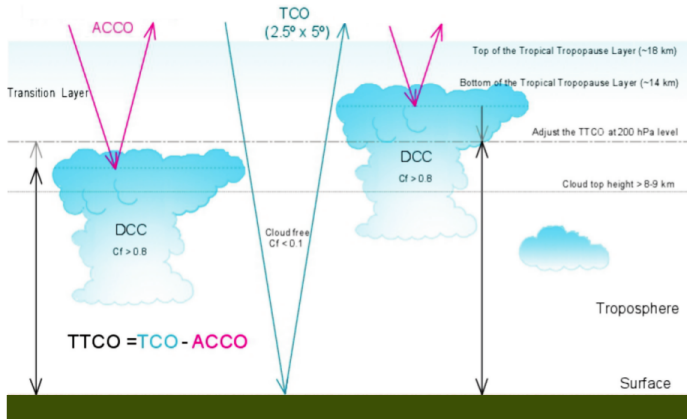


Figure taken from [Leventidou et al., 2016] and modified

Global Fire Emissions Databased (*GFED4*) [van der Werf et al., 2017]

- Derived from satellites measurements (VIRS, ATSR and MODIS).
- Months: August to January of 1997/1998 and 2015/2016.
- Resolution of 0.25° by 0.25° , [20°N , 20°S].

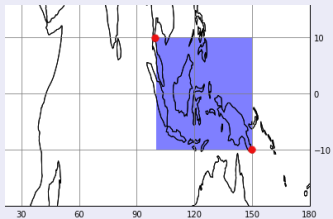
Global Fire Emissions Databased (*GFED4*) [van der Werf et al., 2017]

- Derived from satellites measurements (VIRS, ATSR and MODIS).
- Months: August to January of 1997/1998 and 2015/2016.
- Resolution of 0.25° by 0.25° , [20°N , 20°S].

Particle transport & dispersion model FLEXPART [Stohl et al., 2005]

Lagrangian off-line model version 8.0. Meteorological fields from the European Center of Mid-range Weather Forecast (*ECMWF*)

- Forward simulation upper left corner [10° , 100°] lower right corner [-10° , 150°].
- Resolution: $1^\circ \times 1^\circ$, 20 layers of 1km
- Monthly emissions 2.0×10^6 particles

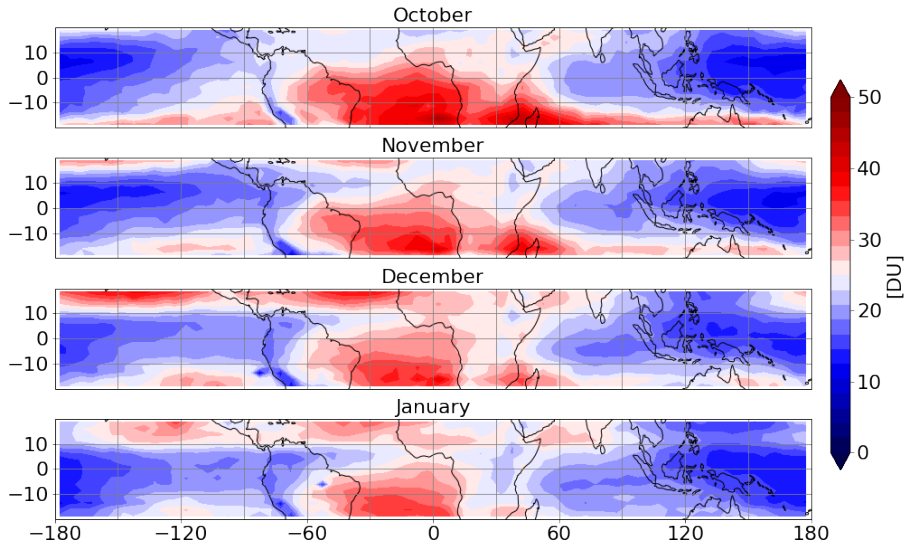


Global Chemistry and transport TM4-EPCL [Daskalakis et al., 2016]

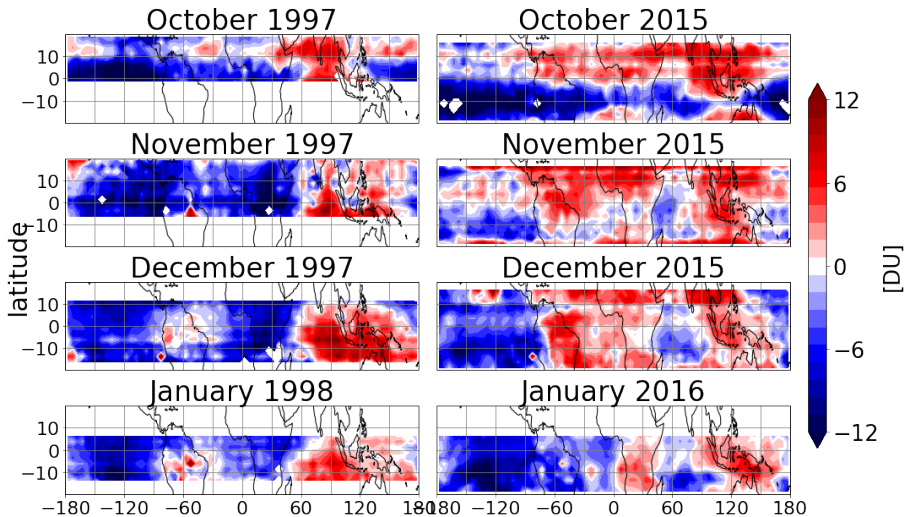
3D offline model. Meteorology from *ECMWF*, anthropogenic and biomass emissions from *ACCMP*, vegetation inventory from *MEGAN-MACC* and *POET2000* for soils and oceans.

- O₃, CO Fields
- Anthropogenic and Biomass Burning scenarios
- Resolution: 2° by 3° and 34 hybrid vertical layers
- Top of troposphere below 150 ppb of O₃ (23rd layer)

Observed ozone monthly mean for the 20 year period

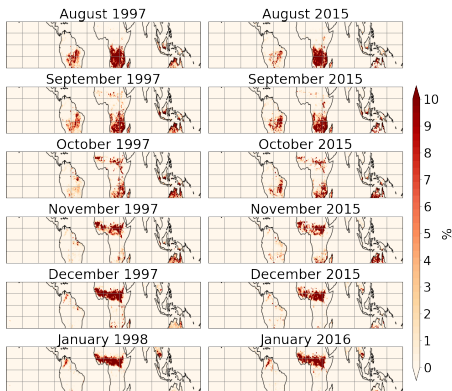


The observed tropospheric ozone anomalies

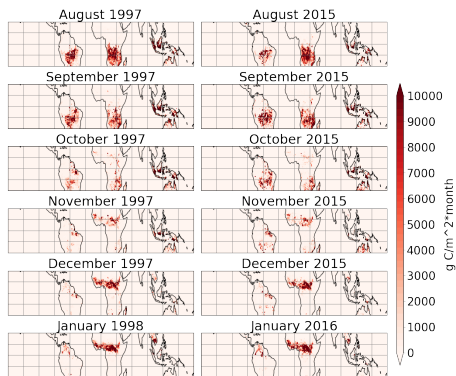


The GFED4 data

Monthly burned area fraction



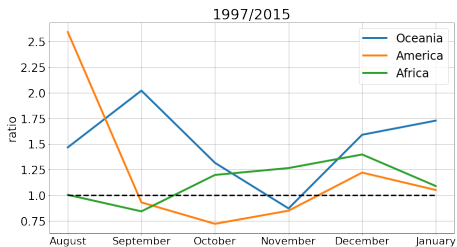
Monthly fire carbon emissions



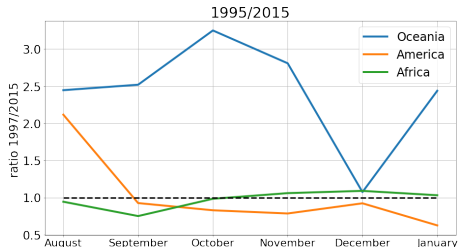
The ratios of GFED4 data

Ratios : 1997/1998 divided by 2015/2016.

Regions: Oceania $[-90^{\circ}, -160^{\circ}]$, Africa $[-20^{\circ}, 50^{\circ}]$, America $[90^{\circ}, 160^{\circ}]$

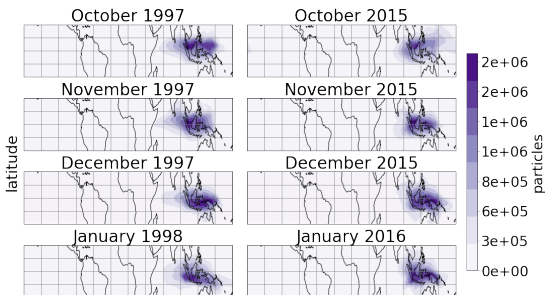
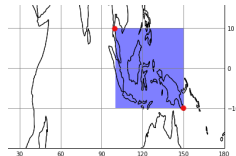


Burned fraction area

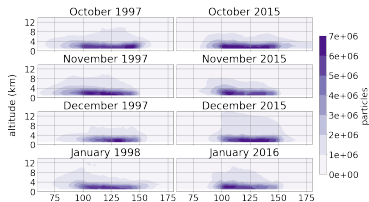


Fire carbon emissions

FLEXPART Transport of ozone



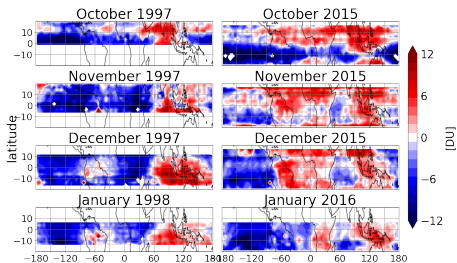
Monthly geographical transport



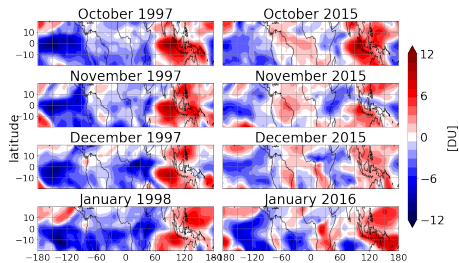
Monthly altitudinal profile

Observed TTCO and TM4-ECPL TTCO

Tropospheric Ozone anomalies



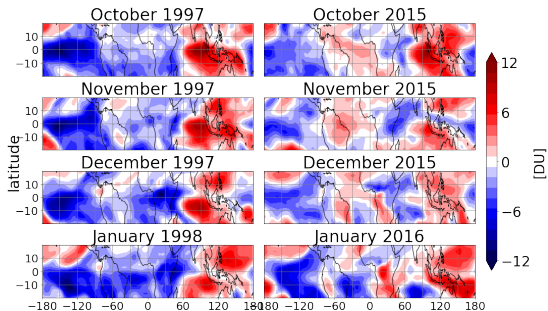
Observed TTCO anomalies



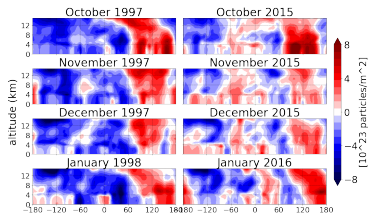
TM4-ECPL TTCO anomalies

TM4-ECPL Changes in the concentration of ozone and precursors

Tropospheric Ozone anomalies



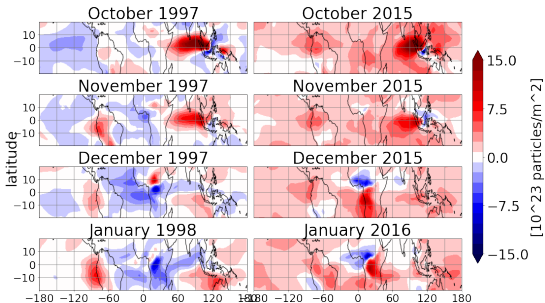
TTCO anomalies



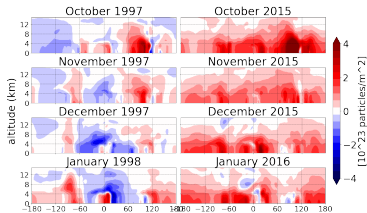
Ozone vertical profile anomalies

TM4-ECPL Changes in the concentration of ozone and precursors

CO anomalies



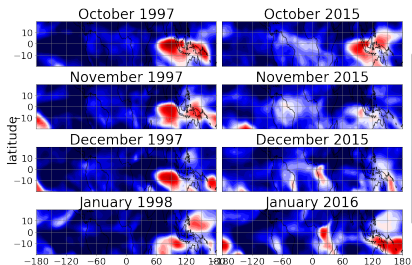
tropospheric carbon monoxide column anomalies



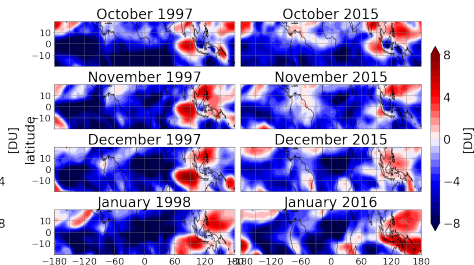
carbon monoxide vertical profile anomalies

TM4-ECPL Biomass Burning and Anthropogenic emissions

Ozone anomalies



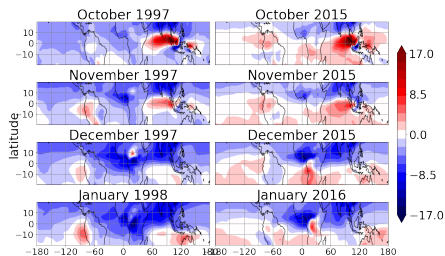
Biomass burning anomalies



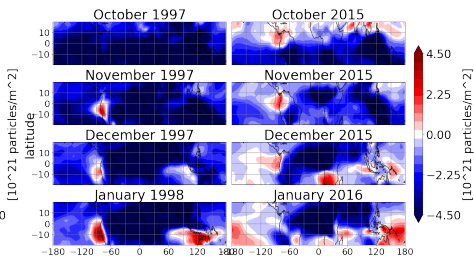
Anthropogenic anomalies

TM4-ECPL Biomass Burning and Anthropogenic emissions

CO anomalies



Biomass Burning anomalies



Anthropogenic anomalies

Summary

- FLEXPART: no difference in transport between years

Summary

- FLEXPART: no difference in transport between years
- Higher burned area and carbon emissions over Oceania in 1997/1998 is consistent with literature

Summary

- FLEXPART: no difference in transport between years
- Higher burned area and carbon emissions over Oceania in 1997/1998 is consistent with literature
- Found that more spread CO anomalies are responsible for 2015/2016 different ozone pattern

Summary

- FLEXPART: no difference in transport between years
- Higher burned area and carbon emissions over Oceania in 1997/1998 is consistent with literature
- Found that more spread CO anomalies are responsible for 2015/2016 different ozone pattern
- The vegetation type influences C and NO_x emissions. High C biomass = higher emissions

Summary

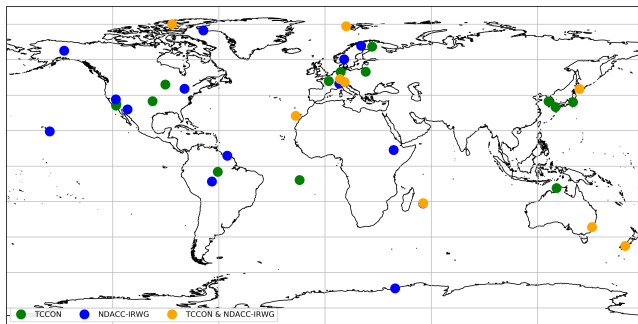
- FLEXPART: no difference in transport between years
- Higher burned area and carbon emissions over Oceania in 1997/1998 is consistent with literature
- Found that more spread CO anomalies are responsible for 2015/2016 different ozone pattern
- The vegetation type influences C and NO_x emissions. High C biomass = higher emissions
- Biomass burning CO values are about 4 times higher than anthropogenic values

Summary

- FLEXPART: no difference in transport between years
- Higher burned area and carbon emissions over Oceania in 1997/1998 is consistent with literature
- Found that more spread CO anomalies are responsible for 2015/2016 different ozone pattern
- The vegetation type influences C and NO_x emissions. High C biomass = higher emissions
- Biomass burning CO values are about 4 times higher than anthropogenic values
- Why the O₃ has the same values for biomass burning and anthropogenic?

PhD: Towards a better understanding on carbon fluxes in the tropics

- We want to study CO₂ fluxes in the Amazon region
- There is little remote sensing measurements retrieving GHGs
- Establish a xCO₂ retrieval for NDACC measurements that are available in:



xCO₂ retrieval from high resolution NDACC measurements
in the 4800 cm⁻¹ region

Introduction

- TCCON operation started in 2004
- NDACC spectra are available in Ny-Ålesund since the early 1990s.
- Use the NDACC spectra for $x\text{CO}_2$ retrieval
- Selected the spectral window in the region between 4780 cm^{-1} and 4800 cm^{-1}
- Used the ggg2014 TCCON retrieval package
- The daily means of the $x\text{CO}_2$ NDACC compared to TCCON and *in situ* data.

Data and Methods

w90 : spectral window centered at 4790 cm^{-1} and 20 cm^{-1} width

From it $x\text{CO}_2$ is calculated:

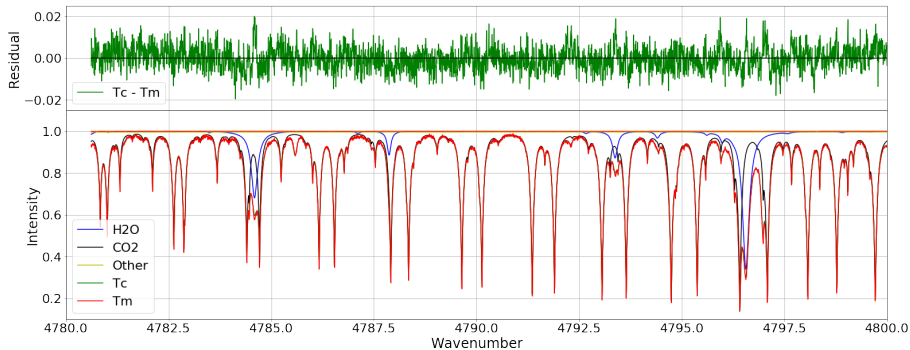
$$x\text{CO}_2 = \frac{VC_{\text{CO}_2}}{VC_{\text{air}}} = \frac{VC_{\text{CO}_2}}{\frac{P_s N_A}{m_{\text{air}}^{\text{dry}} \{g\}} - \frac{VC_{\text{H}_2\text{O}} m_{\text{H}_2\text{O}}}{m_{\text{air}}^{\text{dry}}}}$$

H_2O window at 4576.85 cm^{-1} and 1.90 cm^{-1} width.

Filter criteria: spectra with a SZA $>83^\circ$ and bad spectra.

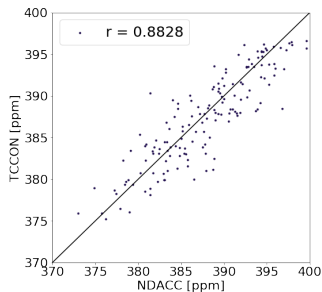
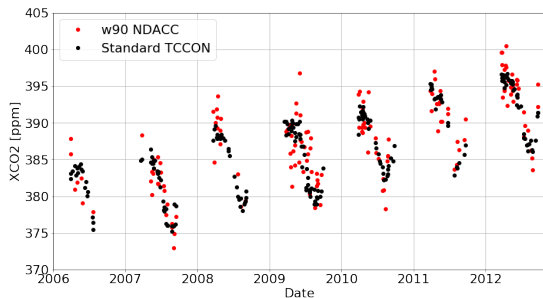
Lastly, daily means weighted with the error of the retrieval was calculated.

Fit and Residual



The fit of the calculated spectra and the residual ($T_m - T_c$) for a typical NDACC spectrum

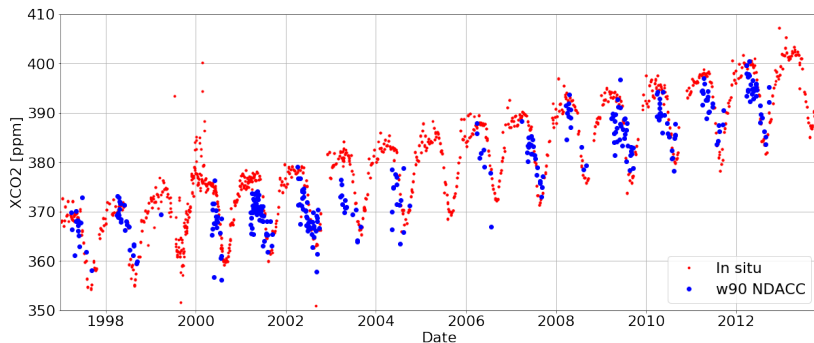
NDACC and TCCON



Daily means of xCO₂ of the TCCON and the weighted daily mean of xCO₂ NDACC

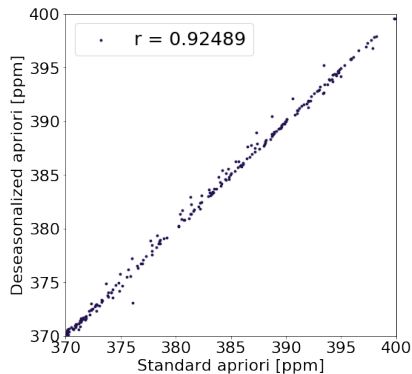
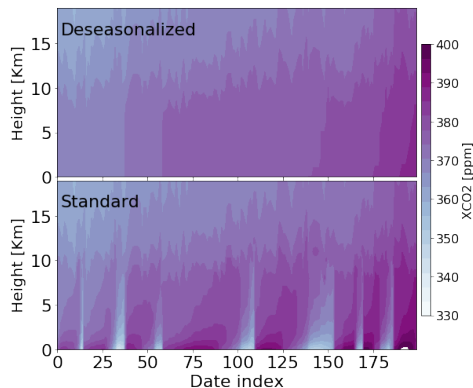
The correlation between TCCON and NDACC

NDACC and *in situ*

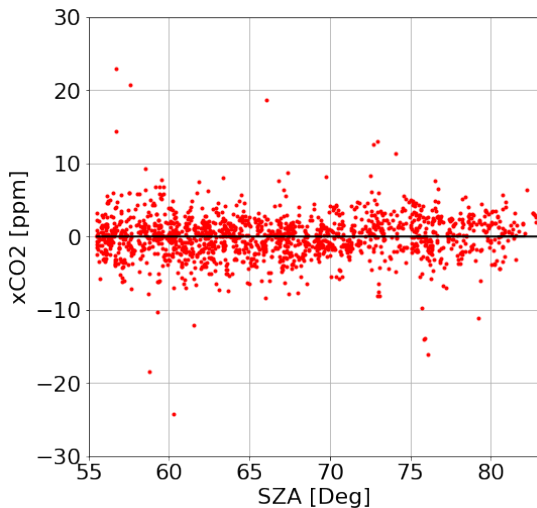


NDACC CO₂ comparison with *in situ* flask data ZEP
[Dlugokencky, E.J.] ([ftp : //aftp.cmdl.noaa.gov/data/trace_gases/co2/flask/surface/](ftp://aftp.cmdl.noaa.gov/data/trace_gases/co2/flask/surface/))

Sensitivity studies: *a Priori*

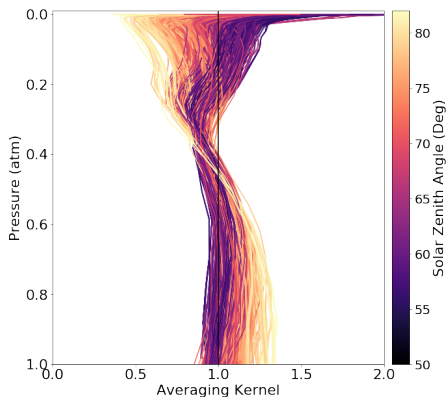


Sensitivity studies: Solar Zenith Angle

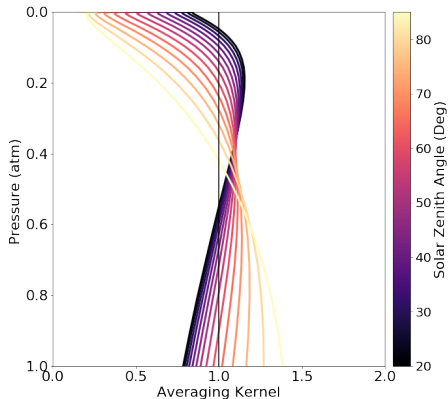


NDACC xCO₂ - monthly mean SZA dependence

Total column averaging kernels



W90 averaging kernels for all
NDACC spectra



The averaging kernels for the
standard TCCON xCO₂

Summary

- Selected a window to retrieve xCO₂ from NDACC measurements.

Summary

- Selected a window to retrieve $x\text{CO}_2$ from NDACC measurements.
- The averaging kernels show good sensitivity near the surface.

Summary

- Selected a window to retrieve $x\text{CO}_2$ from NDACC measurements.
- The averaging kernels show good sensitivity near the surface.
- Performed a comparison of the retrieved $x\text{CO}_2$ to the standard TCCON and *in situ* flask samples.

Summary

- Selected a window to retrieve $x\text{CO}_2$ from NDACC measurements.
- The averaging kernels show good sensitivity near the surface.
- Performed a comparison of the retrieved $x\text{CO}_2$ to the standard TCCON and *in situ* flask samples.
- There is a strong correlation between TCCON $x\text{CO}_2$ and NDACC $x\text{CO}_2$ with $r = 0.8828$.

Summary

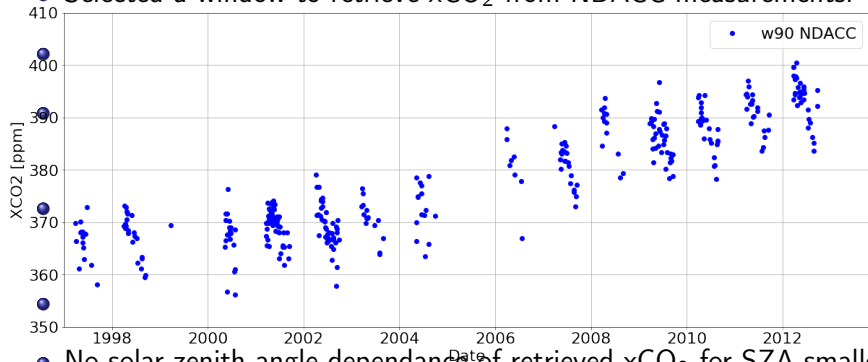
- Selected a window to retrieve $x\text{CO}_2$ from NDACC measurements.
- The averaging kernels show good sensitivity near the surface.
- Performed a comparison of the retrieved $x\text{CO}_2$ to the standard TCCON and *in situ* flask samples.
- There is a strong correlation between TCCON $x\text{CO}_2$ and NDACC $x\text{CO}_2$ with $r = 0.8828$.
- The influence of the *a priori* to the results is negligible.

Summary

- Selected a window to retrieve $x\text{CO}_2$ from NDACC measurements.
- The averaging kernels show good sensitivity near the surface.
- Performed a comparison of the retrieved $x\text{CO}_2$ to the standard TCCON and *in situ* flask samples.
- There is a strong correlation between TCCON $x\text{CO}_2$ and NDACC $x\text{CO}_2$ with $r = 0.8828$.
- The influence of the *a priori* to the results is negligible.
- No solar zenith angle dependence of retrieved $x\text{CO}_2$ for SZA smaller than 83° .

Summary

- Selected a window to retrieve $x\text{CO}_2$ from NDACC measurements.



- No solar zenith angle dependence of retrieved $x\text{CO}_2$ for SZA smaller than 83° .

Outlook

- Apply the same method to spectra from other regions e.g. Porto Velho and Paramaribo.

Outlook

- Apply the same method to spectra from other regions e.g. Porto Velho and Paramaribo.
- Use the retrieved CO₂ to improve flux estimations and diurnal cycles in the Amazon.

Outlook

- Apply the same method to spectra from other regions e.g. Porto Velho and Paramaribo.
- Use the retrieved CO₂ to improve flux estimations and diurnal cycles in the Amazon.
- Compare the results with atmospheric and biospheric models

Outlook

- Apply the same method to spectra from other regions e.g. Porto Velho and Paramaribo.
- Use the retrieved CO₂ to improve flux estimations and diurnal cycles in the Amazon.
- Compare the results with atmospheric and biospheric models
- Using future *in situ* measurements of carbon in rivers in the tropics.

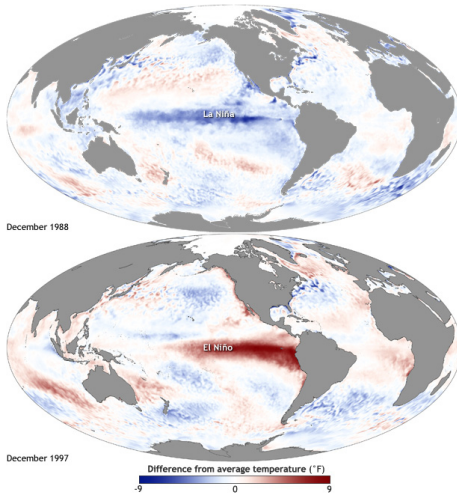
Thank you

References

- Chandra, S., Ziemke, J. R., Min, W., and Read, W. G. (1998).
Effects of 1997-1998 El Niño on tropospheric ozone and water vapor.
Geophysical Research Letters, 25(20):3867–3870.
- Daskalakis, N., Tsigaridis, K., Myriokefalitakis, S., Fanourgakis, G. S., and Kanakidou, M. (2016).
Large Gain in Air Quality Compared to an Alternative Anthropogenic Emissions Scenario.
Atmospheric Chemistry and Physics, 16(15):9771–9784.
- Doherty, R. M., Stevenson, D. S., Johnson, C. E., Collins, W. J., and Sanderson, M. G. (2006).
Tropospheric Ozone and El Niño/Southern Oscillation: Influence of Atmospheric Dynamics, Biomass Burning Emissions, and Future Climate Change.
Journal of Geophysical Research: Atmospheres, 111(D19).
- Fujiwara, M. and Kita, K. (2000).
Seasonal Variation of Tropospheric Ozone in Indonesia Revealed by 5-year Ground-based Observations.
Journal of Geophysical Research: Atmospheres, 105(D2):1879–1888.
- Leventidou, E. (2017).
TROPICAL TROPOSPHERIC OZONE COLUMNS FROM NADIR SATELLITE RETRIEVALS USING THE CONVECTIVE CLOUD DIFFERENTIAL (CCD) TECHNIQUE ON GOME, SCIAMACHY, AND GOME-2 DATA.
PhD Thesis, University Bremen, Bremen.
- Leventidou, E., Eichmann, K.-U., Weber, M., and Burrows, J. P. (2016).
Tropical Tropospheric Ozone Columns from Nadir Retrievals of GOME-1/ERS-2, SCIAMACHY/Envisat, and GOME-2/MetOp-A (1996–2012).
Atmospheric Measurement Techniques, 9(7):3407–3427.
- Ropelewski, C. F. and Halpert, M. S. (1987).
Global and Regional Scale Precipitation Patterns Associated with the El Niño/Southern Oscillation.
Monthly Weather Review, 115(8):1606–1626.
- Stohl, A., Forster, C., Frank, A., Seibert, P., and Wotawa, G. (2005).
Technical Note: The Lagrangian Particle Dispersion Model FLEXPART Version 6.2.
Atmospheric Chemistry and Physics, 5(9):2461–2474.
- Sudo, K. and Takahashi, M. (2001).
Simulation of Tropospheric Ozone Changes during 1997–1998 El Niño: Meteorological Impact on Tropospheric Photochemistry.
Geophysical Research Letters, 28(21):4091–4094.
- Thompson, A. M. (2001).
Tropical Tropospheric Ozone and Biomass Burning.
Science, 291(5511):2128–2132.
- van der Werf, G. R., Randerson, J. T., Giglio, L., van Leeuwen, T. T., Chen, Y., Rogers, B. M., Mu, M., van Marle, M. J. E., Morton, D. C., Collatz, G. J., Yokelson, R. J., and Kasibhatla, P. S. (2017).
Global Fire Emissions Estimates during 1997–2016.
Earth System Science Data, 9(2):697–720.
- Ziemke, J. R., Chandra, S., and Bhartia, P. K. (1998).
Two New Methods for Deriving Tropospheric Column Ozone from TOMS Measurements: Assimilated UARS MLS/HALOE and Convective-Cloud Differential Techniques.
Journal of Geophysical Research: Atmospheres, 103(D17):22115–22127.

Region	Carbon emissions Tg C yr ⁻¹		Contribution of vegetation type to the emissions (%)			
	Mean	Maximum	Savanna	Tropical Forest	Peat	Agriculture
Central America	38	177	45.5	36.7	0.0	15.9
Northern S.A	32	60	71.1	23	0.0	5.9
Southern S.A	291	561	49.3	45.1	0.0	3.2
Northern Africa	451	645	88.3	5.2	0.0	6.5
Southern Africa	669	774	92.4	4.8	0.0	2.7
Indonesia	173	1110	11.2	43.7	42.8	2.2
Australia	116	190	86.3	2.3	0.0	1.5

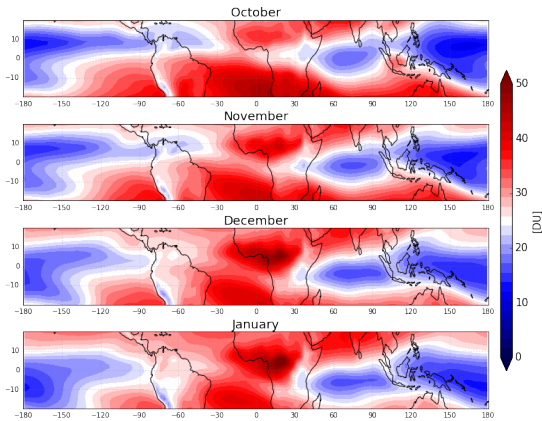
Carbon emissions estimates and the contribution of different fire categories over the 1996 to 2016 study period. Values, some regions, and some vegetation types selected from [van der Werf et al., 2017] page 711.



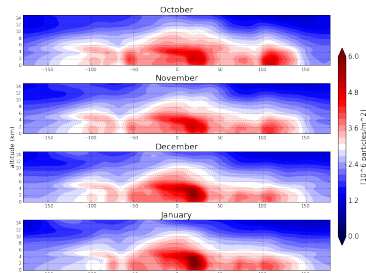
Maps of sea surface temperature anomaly in the Pacific Ocean during a strong La Niña (top, December 1988) and El Niño (bottom, December 1997). Maps by NOAA Climate.gov, based on data provided by NOAA

TM4-ECPL 20 year mean TTCO

Tropospheric Ozone MEAN of 20 years



TTCO MEAN



Ozone vertical profile

$$x_{CO_2} = \frac{VC_{CO_2}}{\frac{P_s N_A}{m_{air}^{dry} \{g\}} - \frac{VC_{H_2O} m_{H_2O}}{m_{air}^{dry}}}$$

VC_{CO_2} is the CO_2 vertical column from the ggg output from w90, VC_{H_2O} is the vertical column from the ggg output for the water window at 4576.85 cm^{-1} of 1.90 cm^{-1} width, P_s is the surface pressure in hPa, $N_A = 6.0221415 \cdot 10^{23}$ molecules/mole, the Avogadro number; $m_{air}^{dry} = 28.9644$ g/mole, mass of dry air; $m_{H_2O} = 18.01534$ g/mole, the mass water and $\{g\} = 9.81 \frac{m}{s^2}$